Guided Tuning of Turbine Blades: A Practical Method to Avoid Operating at Resonance

Loc Duong[1]
Principal Engineer
Hamilton Sundstrand Power Systems,
San Diego, CA 92186
e-mail: loc.duong@hs.utc.com

Kevin D. Murphy
Professor
email: kdm@engr.uconn.edu

Kazem Kazerounian
Professor
e-mail: kazem@engr.uconn.edu

University of Connecticut,
Storrs, CT 06269

In gas turbine applications, forced vibrations of turbine blades under resonant—or nearly resonant—conditions are undesirable. Usually in airfoil design procedures, at least the first three blade modes are required to be free of excitation in the operating speed range. However, not uncommonly, a blade may experience resonance at other higher natural frequencies. In an attempt to avoid resonant oscillations, the structural frequencies are tuned away from the excitation frequencies by changing the geometry of the blade. The typical iterative design process—of adding and removing material through restacking the airfoil sections—is laborious and in no way assures an optimal design. In response to the need for an effective and fast methodology, the guided tuning of turbine blades method (GTTB) is developed and presented in this paper. A practical tuning technique, the GTTB method is based on structural perturbations to the mass and stiffness at critical locations, as determined by the methodology described herein. This shifts the excited natural frequency out of the operating speed range, while leaving the other structural frequencies largely undisturbed. The methodology is demonstrated here in the redesign of an actual turbine blade. The numerical results are experimentally validated using a laser vibrometer. The results indicate that the proposed method is not computationally intensive and renders effective results that jibe with experiments. [DOI: 10.1115/1.4024761]

1 Introduction

In gas turbine applications, rotating blades that operate under resonant conditions may result in catastrophic failures. The most common excitation source is the nonuniform pressure distribution caused by gas flow around obstacles such as an upstream static guide vane of a nozzle. If there are N evenly spaced vanes, a downstream blade is excited N times per rotor revolution (N engine orders). Other excitation sources could stem from mechanical origins such as bearing support alignment and residual rotor bow. Usually their influence may be significant as high as up to the fourth engine order. A preliminary airfoil design is usually tuned for the first three or four natural frequencies in order to avoid resonance with these low engine orders. However, a blade may experience resonance at the vane passing frequency, which is a high engine order. This excited natural frequency is required to be shifted outside of the operating speed range without greatly disturbing the other frequencies.

In the open literature there has been a good deal of work on mistuning frequency/mode calculations [1–3]. These commonly deal with random structural perturbations away from the idealized symmetric system, including the use of intentional mistuning patterns to mitigate the harmful effects of random mistuning. While these works are relevant, they do not suggest how to avoid the problem of resonance.

There are several options for avoiding large amplitude vibrations associated with resonance. The operating speed may be changed to avoid a resonance condition, although this is a very restrictive option. Alternatively, a platform damper may be attached to the blade to reduce the mean amplitude (and stress level) [4–6]. Such dampers are widely employed in industry. However, they become less effective at a high frequency.

Alternatively, one may redesign the blade itself, as recently suggested in Ref. [7]. This moves the structural frequencies away from the engine order excitation, avoiding resonance. This is the approach commonly taken by industry, although the specifics of their redesign procedures are not publically available. It was claimed in patents [8,9] that blade tuning was achieved through filling a recess at the blade tip with a material, which is different from that of the blade material. Journal publications that develop clear redesign methodologies are scarce. This void in the open literature is part of the motivation for the present paper. The idea here is to develop and demonstrate a consistent methodology that "tunes" the blade geometry such that the natural frequency changes and pushes the resonance condition out of the operating speed range, as seen in Fig. 1. The task of tuning the blade is further complicated by the following additional constraints:

1. Redesigning the geometry changes all of the frequencies (eigenvalues). Thus, while a certain geometry change might move the ith frequency out of the operating range, it might also (inadvertently) move the jth frequency into the operating range. This undermines the tuning process. As such, the goal is to move the desired frequency while leaving the others largely unchanged. In Fig. 1, this would mean moving point A to A′, while not appreciably changing the fundamental frequencies represented by B, C, D, and E.
2. The preliminary airfoil geometry, tuned for fundamental modes, was developed to ensure good aerodynamic performance. As such, changes to the geometry in this tuning process should not drastically impact the lift/drag characteristics of the blade.
3. It is also assumed that modification to the upstream hardware, for instance, the number of vanes on the stator or the number of fuel nozzles, is not an option.

Using classical eigenvalue perturbation theory, the perturbations are applied in such a way as to limit the changes to other frequencies, as required by item 1. However, this method does not ensure that item 2 is satisfied. Such an assurance would require a coupled fluid-structure model. This high degree of specificity is outside the scope of this work, whose aim is to develop and demonstrate a redesign process to resolve a structural vibration problem.

The methodology is as follows: (i) The various engine order excitations are identified. (ii) Using a finite element description of the original blade geometry (pretuning), the free vibration eigenvalue problem is solved. This gives the natural frequencies and mode shapes. (iii) A Campbell diagram is created, identifying all resonant conditions but especially the one(s) inside the operating speed range. The resonant conditions inside the operating range are referred to as the *offending frequencies*. (iv) For all resonances inside the operating range, the maxima of their associated mode shape(s) are identified. (v) A small amount of material is added to or removed from the blade at the maxima of the offending mode

[1]Corresponding author.
Contributed by the Design Engineering Division of ASME for publication in the Journal of Vibration and Acoustics. Manuscript received April 30, 2012; final manuscript received May 14, 2013; published online June 19, 2013. Assoc. Editor: Yukio Ishida.

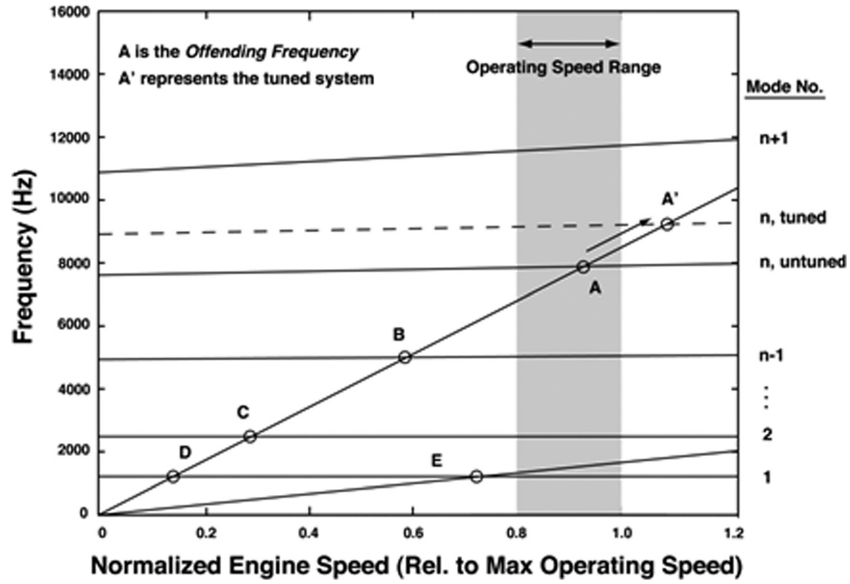

Fig. 1 The effects of blade tuning in the Campbell diagram

(see the previous step). This changes the mass and stiffness matrices and; hence, impacts the natural frequencies. However, because it takes place at a modal peak, the change in the eigensolution is most noticeable in the offending frequency/mode; there is a smaller change in the other frequencies/modes. The process returns to step (ii) and the process continues until the offending frequency is pushed outside of the operating range.

2 Analytical Justification

The fifth step of the GTTB method is to add or subtract material from a blade in *strategic locations* in order to change the offending frequency, pushing the resonance condition outside of the operating range of the engine, while leaving the other frequencies largely undisturbed.

The eigenvalues and eigenvectors for a free vibration problem are numerically obtained from the standard eigenvalue problem

$$-\lambda_0[\mathbf{M}]\{\phi_0\} + [\mathbf{K}]\{\phi_0\} = 0 \quad (1)$$

where ϕ, $[\mathbf{M}]$, and $[\mathbf{K}]$ are normal modes, mass, and stiffness matrices, respectively.

As usual, the frequencies squared are the individual eigenvalues. Adding or removing mass makes small changes to specific terms of the mass and stiffness matrix; these terms must correspond to the nodes at the physical location on the blade that is being altered. Introducing these small perturbations $[\delta\mathbf{K}]$ and $[\delta\mathbf{M}]$ to the net stiffness and mass yields

$$[\mathbf{K}] = [\mathbf{K}_O] + [\delta\mathbf{K}] \quad (2)$$

and

$$[\mathbf{M}] = [\mathbf{M}_O] + [\delta\mathbf{M}] \quad (3)$$

The subscript (O) in the preceding equations refers to the mass and stiffness matrices from the previous iteration (or the unperturbed system if this is the first iteration of the GTTB process). It is also assumed that nonzero elements of the perturbation matrices are small in comparison to the same elements in the original mass and stiffness matrices. Because these perturbations are small, it can be assumed that the ith eigenvalue and eigenvector undergo small changes

$$\lambda_i = \lambda_{oi} + \delta\lambda_i \quad (4)$$

and

$$\phi_i = \phi_{oi} + \delta\phi_i \quad (5)$$

In addition, provided the original mass and stiffness matrices are symmetric and positive definite, we have the following:

$$\phi_{oi}^T[\mathbf{M}_O]\phi_{oi} = 1 \quad (6)$$

and

$$\phi_{oi}^T[\mathbf{K}_O]\phi_{oi} = \lambda_{oi} = \omega_{oi}^2 \quad (7)$$

With these definitions, it can be shown [10,11] that the perturbed eigenvalues and eigenvectors may be expressed as

$$\lambda_i = \lambda_{oi} + \left(\phi_{oi}^T[\delta\mathbf{K}]\phi_{oi} - \lambda_{oi}\phi_{oi}^T[\delta\mathbf{M}]\phi_{oi}\right) \quad (8)$$

$$\phi_i = \phi_{oi} - (1/2)\left\{\phi_{oi}^T[\delta\mathbf{M}]\phi_{oi}\right\}\phi_{oi} + \sum_{j=1,N(j\neq i)} \left(\phi_{oj}^T\{[\delta\mathbf{K}] - \lambda_{oi}[\delta M]\}\phi_{oi}\right)\phi_{oj}/(\lambda_{oj} - \lambda_{oi}) \quad (9)$$

The goal is to add or subtract mass to produce a sufficiently large change in the offending eigenvalue. To quantify the total change in the eigenvalue, the total derivative is taken

$$d\lambda_i = \frac{d\lambda_i}{\partial k_{kl}}dk_{kl} + \frac{\partial\lambda_i}{\partial m_{kl}}dm_{kl} \quad (10)$$

which requires that the two partial derivatives be evaluated. These are also referred to as the sensitivities of λ_i and ϕ_i with respect to perturbations in $[\mathbf{K}]$ and $[\mathbf{M}]$. These derivatives are

$$\frac{\partial\lambda_i}{\partial k_{kl}} = \frac{\partial}{\partial k_{kl}}\left(\lambda_{oi} + \left(\phi_{oi}^T[\delta\mathbf{K}]\phi_{oi} - \lambda_{oi}\phi_{oi}^T[\delta\mathbf{M}]\phi_{oi}\right)\right)$$

$$\frac{\partial\lambda_i}{\partial k_{kl}} = \frac{\partial}{\partial k_{kl}}\left(\phi_{oi}^T[\delta\mathbf{K}]\phi_{oi}\right) = \frac{\partial}{\partial k_{kl}}(\phi_{oi}\phi_{oi})^T[\delta\mathbf{K}]$$

With the symmetric $[\mathbf{K}]$ matrix, a partial with respect to k_{kl} term will change the k and l elements of the vector, leaving

$$\frac{\partial\lambda_i}{\partial k_{kl}} = (2 - \delta_{kl})\phi_{oi(k)}\phi_{oi(l)} \quad (11)$$

where δ_{kl} is the Kronecker δ and the parenthetical subscript refers to the specific element within the eigenvector.

Similarly, for changes in the mass we obtain $\partial\lambda_i/\partial m_{kl}$

$$\frac{\partial\lambda_i}{\partial m_{kl}} = \frac{\partial}{\partial m_{kl}}\left(\lambda_{oi} + \left(\phi_{oi}^T[\delta\mathbf{K}]\phi_{oi} - \lambda_{oi}\phi_{oi}^T[\delta\mathbf{M}]\phi_{oi}\right)\right)$$

and

$$\frac{\partial\lambda_i}{\partial m_{kl}} = (2-\delta_{kl})\lambda_{oi}\phi_{oi(k)}\phi_{oi(l)} \tag{12}$$

To produce a change in a specific eigenvalue λ_i, Eq. (11) suggests that one should examine the ith mode shape for an antinode (choose the klth matrix elements to correspond to a spatial maximum in ϕ). It is at this location that the stiffness should be enhanced, since it produces the largest change to the eigenvalue per unit stiffness perturbed. A similar observation is also true for the perturbation in mass, as indicated by Eq. (12). The eigenvalue perturbation bounds are scaled by the amplitude of the mode shape.

While the perturbation of the eigenvalue λ_i depends solely on the perturbation of the [**K**] and [**M**] matrices, the perturbation in the eigenvector ϕ_i depends on the perturbations in [**K**] and [**M**] but also on the differences between λ_i and the other eigenvalues; see Eq. (9). However, the focus here is on changes in the frequency, since that dictates resonance. Changes in mode shapes are incidental.

Equation (8) provides a quantitative estimate of the new frequency for a given perturbation in [**K**] and [**M**]. Ideally, the problem would be solved in reverse. The required change in λ_i would be specified and the amount of material to be added/subtracted would be calculated. This would be the 'holy grail,' knowing exactly where to add material and by how much. An actual structure is simply too complex, meaning that there may be a large number of geometry changes that could yield the desired change in λ_i. To circumvent this uniqueness issue, an iterative approach is taken. It is clear where material should be added/subtracted: at antinodes of the mode shape associated with the offending frequency. A small geometric change is made in this vicinity and the eigenvalues are recalculated. If the updated eigenvalue hasn't changed by a satisfactory amount, the geometry is perturbed from this updated configuration and the process is repeated until the offending frequency falls outside of the operating range.

At this point, it is worth briefly discussing the specialized (but highly studied) case of symmetry breaking and mode localization [12,13]. Let us assume that the offending frequency is associated with a highly localized mode. In this case, the choice of where to add/remove material becomes particularly easy since the modal peak is pronounced. The other half of the problem is the eigenvalue veering that often accompanies mode localization [14,15]. In the parameter region where the veering occurs, the strongly coupled (veering) eigenvalues are close in value. Thus, both would probably be "offending frequencies." Therefore, if one increases and moves outside of the operating speed range, the other will also likely fall outside of the operating speed range.

3 Physical Example

In practice, it is preferable to subtract mass in order to shift a resonant frequency above the upper bound of the operating speed range to avoid excitation during engine speed up and ramp down. Additionally, it circumvents the negative impact on blade fir tree stress, on rotor inertia, and on blade-off containment requirements caused by mass addition.

The model for this blade is shown in Fig. 2(*a*); the actual blade (sitting in the test fixture) is shown in Fig. 5. The blade has a modulus and density of $E = 207$ GPa and $\rho = 7.8 \times 10^3$ kg/m^3, respectively. The finite element model uses tetrahedron elements and each node has six degrees of freedom. The fir tree structure, at the hub of the rotor, is fully fixed. The results of the first three steps of the GTTB process are summarized in the Campbell diagram of Fig. 1. This indicates that the structure has distinct eigenvalues and that the nth frequency (labeled "A") is in the operating speed range, making it resonant. This is referred to as the offending frequency. Beginning at step four, the nth mode shape ϕ_n is generated and examined for maxima. This is shown in Fig. 2(*b*). The yellow/red areas correspond to modal peaks, while blue areas have little displacement. Here, there is one principle modal peak (red) and two secondary peaks (yellow), as labeled in Fig. 2(*b*). Although all three areas may be perturbed, the focus here will remain on the primary maxima.

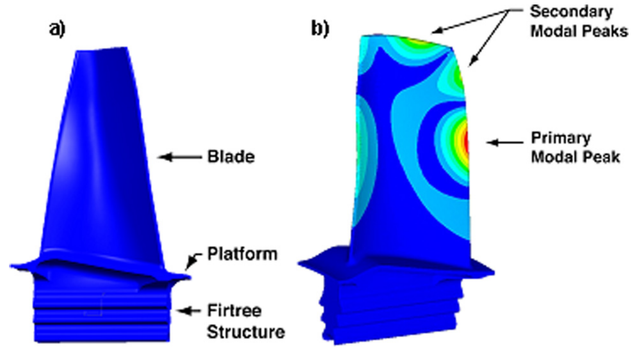

Fig. 2 Turbine blade

Step number five requires that material perturbations be imposed on the structure to shift this resonant frequency from the current position inside the operating range to a position outside of the operating speed range (to point A′). To accomplish this particular shift (going from A to A′) a frequency change of approximately 8% is required.

To ensure the consistency and integrity of the analysis, the finite element mesh was never changed. To remove material from a region, the density and modulus of the material in that region are set to zero. In this particular case, the primary modal peak is broken into three bands of elements, as shown in Fig. 3, and identified as V_1, V_2, and V_3. Initially, only volume one (V_1) is removed, by zeroing out these material properties (E and ρ). This changes the frequency by slightly more than 3% and is insufficient. Removing volume two (V_2) increases the net change to 5.5%, which is still insufficient. Volume three (V_3) is then removed and the total percent change in the nth frequency is approximately 8.25%. These

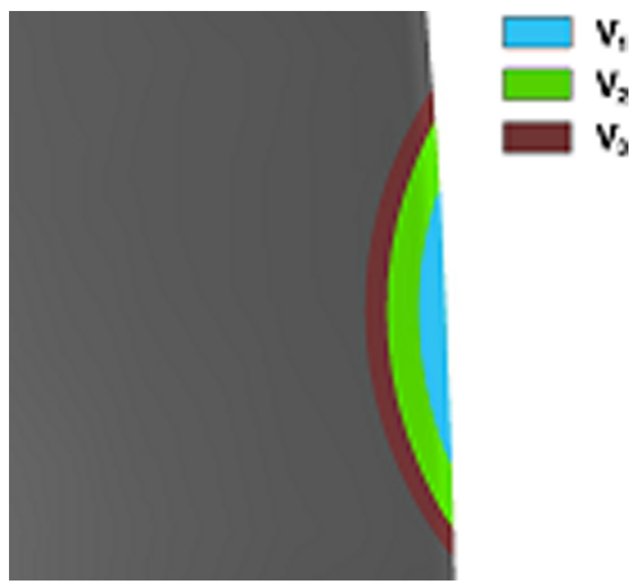

Fig. 3 The trailing edge of the blade with subvolumes at the primary modal peak

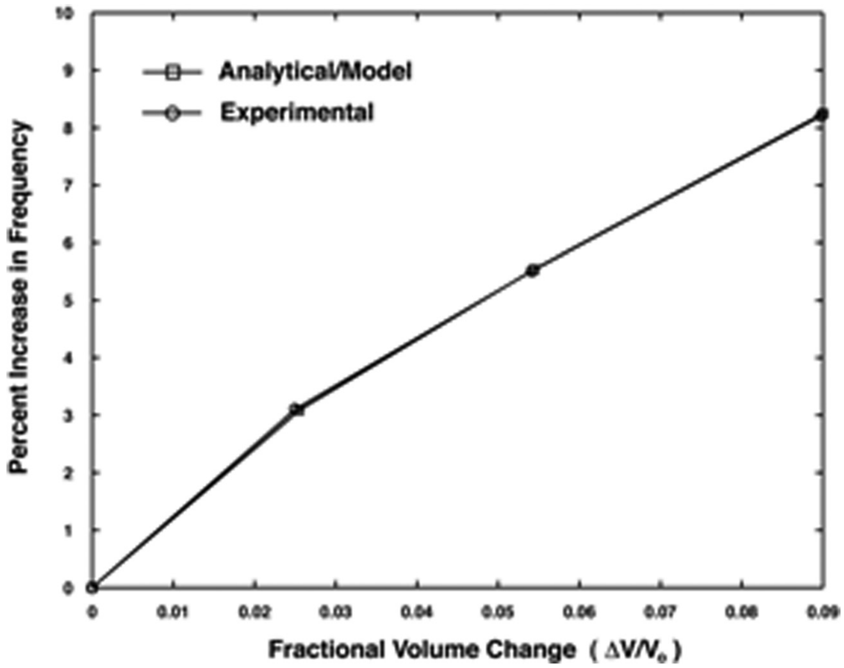

Fig. 4 Percent of the frequency shift as a function of material volume removal at the primary modal peak. The model predictions and experimental results are both shown.

iterative improvements are shown in Fig. 4. This structural redesign pushes point A to A′ in the Campbell diagram, while leaving the other frequencies largely undisturbed.

4 Experimental Validation

The test configuration is shown in Fig. 5. The fir tree portion of the turbine blade is clamped in a rigid support fixture, which, in turn, is clamped onto a shake table. The blade is acoustically excited by a speaker that is placed just behind the blade. The speaker is driven by an amplifier and a wave form generator. The excitation is sinusoidal and the frequency is varied over the course of the tests. The sensor is a scanning laser vibrometer. In the nonscanning mode, this emits light toward one point on the test object (the blade) and measures the phase difference from the projected and reflected wave. This gives the velocity of that point. In the scanning mode, the target point is varied. Provided the vibrations are reasonably small and the response linear, the velocity distribution and the mode shape are the same (just 90° out of phase). Hence, the measured field is the mode shape.

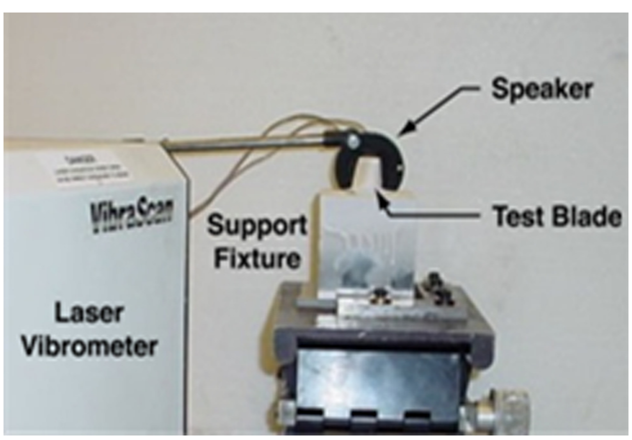

Fig. 5 The test configuration, including the laser vibrometer, shaker table, support fixture, and blade

The experimental objective is to verify two things. First, the natural frequency and mode shape of the untuned blade must be verified. The second is to verify the natural frequency and mode shape of the tuned blade after the previously specified amount of material has been removed.

The first test involves adjusting the excitation frequency (in the vicinity of the anticipated *n*th natural frequency) until a resonance condition exists. This test showed that the actual frequency of the untuned system differed from the model predicted frequency by approximately 0.1%. This is in excellent agreement. The associated mode shape is shown in Fig. 6(*a*). The modal peaks correspond to the red zones. This agrees favorably with the model predicted mode shape in Fig. 2(*b*).

The next experiment follows the iterative approach taken in the simulations. Material is machined off of the blade, at the prescribed location, in small amounts. First, volume V_1 (see Fig. 3) is removed and the frequency is measured. This is followed by V_2

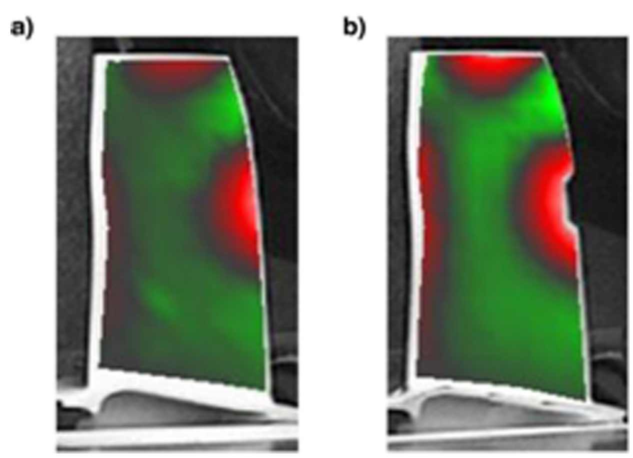

Fig. 6 (*a*) Measured mode shape of the baseline blade at point A in the Campbell diagram. (*b*) The mode shape of the tuned blade after the second iteration (with a 5.5% change in the frequency).

and V_3. In all cases, the measured percent increase in the frequency differed from the predicted percent increase in the frequency by less than 0.1%. A head-to-head comparison of the model results versus the experimental results is shown in Fig. 4. Additionally, the experimental mode shape after the second iteration is shown in Fig. 6(*b*). There is clear agreement between the model and experiment.

5 Conclusions

At certain operating speeds, upstream components (e.g., stators) can induce resonant vibrations in flexible turbine blades. To prevent these situations the blades are often redesigned, such that their resonance conditions fall outside of the operating range of the engine. These redesign efforts are often done heuristically. In this paper, a new approach to turbine blade redesign, referred to as the guided tuning of turbine blades (GTTB), is described. This technique is demonstrated in the redesign of an actual turbine blade. The experimental evidence confirms the results produced by the analysis. The test also indicated that the frequency sensitivity of the other modes, particularly to those adjacent to the tuned frequency, is on the order of less than 1%.

The GTTB methodology uses general results from the perturbation solution to the eigenvalue problem to provide a strategy for the redesign process. Specifically, it requires that the user identify the offending frequency and then add or remove mass from a modal peak (antinode) of the associated mode. This produces a large change in the offending frequency, while leaving the other frequencies largely undisturbed. This can be done iteratively, until the offending frequency leaves the operating speed of the engine. Of course, since the blade profile is changed during this redesign, one should re-examine the flow characteristics of the blade in order to ensure that the redesign has not negatively impacted its aerodynamic performance. Since a typical airfoil is designed for the peak pressure ratio between the pressure side and the suction side on the first two thirds of the blade chord, it is expected that a modification to the blade trailing edge would not have a significant impact on the blade performance. In order to reduce the stress concentration effect, the modified trailing edge profile needs to be smoothly recontoured.

Acknowledgment

The authors wish to thank Hamilton Sundstrand Power Systems management for permission to use some of the experimental results in this paper.

References

[1] Laxadle, D., Thouverez, F., Sinou, J.-J., Lombard, J.-P., and Baumhauer, S., 2007, "Mistuning Identification and Model Updating of an Industrial Blisk," Int. Journal of Rotating Machinery, **2007**, p. 17289.

[2] Hemberger, D., Filsinger, D., and Bauer, H.-J., 2012, "Investigations on Maximum Amplitude Amplification Factor of Real Mistuned Bladed Structures," Proceedings of the ASME Turbo Expo 2012, Copenhagen, June 11–15, ASME Paper No. GT2012-68084.

[3] Choi, B.-K., Lentz, J., Rivas-Guerra, A. J., and Mignolet, M. P., 2003, "Optimization of Intentional Mistuning Patterns for the Reduction of the Forced Response Effects of Unintentional Mistuning: Formulation and Assessment," ASME J. Eng. Gas Turbines Power, **125**, pp. 131–140.

[4] Yang, B. D. and Menq, C. H., 1997, "Modeling of Friction Contact and Its Application to the Design of Shroud Contact," ASME J. Eng. Gas Turbines Power, **119**, pp. 958–963.

[5] Griffin, J. H. and Labelle, R. F., 1996, "A Rational Method for Optimizing Shroud Damping," ASME Paper No. 96-GT-402.

[6] Sanliturk, K. Y., Ewins, D. J., and Stanbridge, A. B., 2003, "Underplatform Dampers for Turbine Blades: Theoretical Modeling, Analysis, and Comparison With Experimental Data," ASME J. Eng. Gas Turbines Power, **123**, pp. 919–929.

[7] Ewins, D. J., 2010, "Control of Vibration and Resonance in Aero Engines and Rotating Machinery—An Overview," Int. J. Pressure Vessels Piping, **87**, pp. 504–510.

[8] Walter, D., and Christoph, R., 2006, "Frequency Tuning Method of a Turbine Blade and Turbine Blade," European Patent No. EP1640562(A1).

[9] Ellis, D. H., 1978, "Composite Reinforcement of Metallic Airfoils," U.S. Patent No. US4118147.

[10] Fonseca, I. M. and Bainum, P. M., 2001, "Large Space Structure Integrated Structural and Control Optimization, Using Analytical Sensitivity Analysis," J. Guid. ControlDyn., **24**(5), pp. 978–982.

[11] Duong, L., Kazerounian, K., and Murphy, K. D., 2008, "An Approach on Tuning Frequency of a Rotating Blade," ASME Paper No. DETC2008-49442.

[12] Pierre, C. and Dowell, E. H., 1987, "Localization of Vibrations by Structural Irregularity," J. Sound Vib., **114**(3), pp. 549–564.

[13] King, M. E. and Vakakis, A. F., 1995, "Asymptotic Analysis of Nonlinear Mode Localization in a Class of Coupled Continuous Structures," Int. J. Solids Struct., **32**(8), pp. 1161–1177.

[14] Perkins, N. C. and Mote, C. D., Jr., 1986, "Comments on Curve Veering in Eigenvalue Problems," J. Sound Vib., **106**(3), pp. 451–463.

[15] Plaut, R. H., Murphy, K. D., and Virgin, L. N., 1995, "Curve and Surface Veering for a Braced Column," J. Sound Vib., **187**(5), pp. 879–885.